Published in final edited form as:
Environ Sci Nano. 2014 December 1; 1(6): 95–603. doi:10.1039/C4EN00102H.

Towards Elucidating the Effects of Purified MWCNTs on Human Lung Epithelial cells

Chenbo Dong[#],
Department of Chemical Engineering, West Virginia University, Morgantown WV, 26506, USA

Reem Eldawud[#],
Department of Chemical Engineering, West Virginia University, Morgantown WV, 26506, USA

Dr. Linda M. Sargent,
National Institute for Occupational Safety and Health, Morgantown WV, 26505, USA

Dr. Michael L. Kashon,
National Institute for Occupational Safety and Health, Morgantown WV, 26505, USA

David Lowry,
National Institute for Occupational Safety and Health, Morgantown WV, 26505, USA

Prof. Yon Rojanasakul, and
Department of Basic Pharmaceutical Sciences, West Virginia University, Morgantown WV, 26506, USA

Prof. Cerasela Zoica Dinu
Department of Chemical Engineering, West Virginia University, Morgantown WV, 26506, USA

Cerasela Zoica Dinu: cerasela-zoica.dinu@mail.wvu.edu

Abstract

Toxicity of engineered nanomaterials is associated with their inherent properties, both physical and chemical. Recent studies have shown that exposure to multi-walled carbon nanotubes (MWCNTs) promotes tumors and tumor-associated pathologies and lead to carcinogenesis in model *in vivo* systems. Here in we examined the potential of purified MWCNTs used at occupationally relevant exposure doses for particles not otherwise regulated to affect human lung epithelial cells. The uptake of the purified MWCNTs was evaluated using fluorescence activated cell sorting (FACS), while the effects on cell fate were assessed using 2- (4-iodophenyl) - 3- (4-nitrophenyl) - 5-(2, 4-disulfophenyl) -2H-tetrazolium salt colorimetric assay, cell cycle and

Correspondence to: Cerasela Zoica Dinu, cerasela-zoica.dinu@mail.wvu.edu.
[#]Equally contributing authors

Author contribution
C.D and R.E have performed the vast majority of the experiments and drafted the manuscript. D.L. performed the cellular exposure to MWCNTs for the elasticity analysis; L.M.S has supervised these experiments. M.L.K. has performed the cell cycle and cell elasticity statistical analysis. Y.R. provided guidance in the design of the cell activity assays. C.Z.D has designed the experiments and finalized the manuscript. All authors have approved the manuscript.

Conflict of Interests
Research findings and conclusions are those of the authors and do not necessarily represent the views of the National Institute for Occupational Safety and Health. The authors declare no competing financial interest.

nanoindentation. Our results showed that exposure to MWCNTs reduced cell metabolic activity and induced cell cycle arrest. Our analysis further emphasized that MWCNTs-induced cellular fate results from multiple types of interactions that could be analyzed by means of intracellular biomechanical changes and are pivotal in understanding the underlying MWCNTs-induced cell transformation.

Keywords

Carbon nanotubes; cyto-genotoxic effects; cell cycle arrest; biomechanical changes

1. Introduction

Multi-walled carbon nanotubes (MWCNTs) aspect-ratio and their ease of functionalization with drugs and biomolecules were recently shown to increase their cellular delivery for applications in diagnostics,[1] drug delivery[2] and cancer therapies.[3, 4] Studies also showed that dispersion stability and loading conditions could influence MWCNTs-induced therapeutic effects as well as the efficiency of a loaded drug.[5] However, such studies failed to reduce the MWCNTs-induced inflammatory effects[6] or to resolve the overall mechanisms of toxicity associated with MWCNTs cellular uptake.[7–10]

Purification via strong acids oxidation was recently used as a mean to increase nanotube dispersity and modify both their chemical and physical properties.[11] Strong acid oxidation shortened the MWCNTs by cutting them at their defect sites, removing impurities and inducing O-derivated functionalities.[12] Such purified MWCNTs had lower immunological toxicity on BALB/c mice when compared to their impure counterparts (i.e, MWCNTs containing Fe on their external or internal walls).[13] Complementary, shorter MWCNTs were shown to illicit reduced inflammatory and toxicity responses in the pleural cavity of the mice.[14] Further, exposure to shorter and purified MWCNTs was shown to lead to changes in the mechanical properties of epithelial cells[15] used previously as models for nanomaterial assessment.[8] However, it is still subject to debate to what extent such purified forms of MWCNTs influence cell fate and what are the resulting nanotube-induced cell transformations that could lead to toxicity and cancer development. Failure to assess such effects could potentially jeopardize the implementation of the purified forms in MWCNTs-based nanotherapeutics.[16]

Combining conventional biocellular and nanoindentation assays[15] we proposed to unravel the cellular changes induced by exposure to purified MWCNTs, all as a function of the nanomaterial physical and chemical properties. Since the respiratory tract is the primary route of exposure by inhalation, [17] lung-derived BEAS-2B cells were considered a suitable model system to evaluate MWCNTs-induced cellular changes[8, 15] with the exposure dose being determined by extrapolation of *in vivo* studies mimicking human exposure for 20 weeks at Occupational Safety and Health Administration (OSHA) permissible limits for particles not otherwise regulated.[8]

2. Materials and Methods

2.1 Multi-walled carbon nanotubes (MWCNTs) purification

MWCNTs (Nanolab Inc., 100 mg) were purified by ultrasonication (Branson 2510, Fisher Scientific) in a strong mixture of sulfuric (Fisher Scientific, 96.4%) and nitric (Fisher Scientific, 69.5%) acids (volume ratio 3:1) for 1 h at a temperature of about 23°C. Upon time elapsed, the mixture was diluted in deionized water (DI water) and filtered through a polycarbonate membrane (Fisher Scientific, GTTP 0.2 μm); the process was repeated several times to remove acid residues or impurities. Purified MWCNTs were collected on a fresh GTTP filter, dried, and stored at room temperature.

2.2 MWCNTs characterization

Fourier Transform Infrared Spectroscopy (FTIR, Digilab FTS 7000) equipped with diamond Attenuated Total Reflection (ATR) crystal was used to investigate the chemical properties of pristine and purified MWCNTs. Scans ranging from 1000 to 4000 cm^{-1} were collected.

Morphology and elemental quantitative analyses of pristine and purified MWCNTs (1 mg/mL sample on silica wafer) were performed on a Hitachi S-4700 Field Emission Scanning Electron Microscope (Hitachi High-Technologies Corporation) containing a S-4700 detector combining secondary (SE) and backscattered (BSE) electron detection and operating at 20 KV. For Energy Dispersive X-Ray Spectroscopy (EDX) results are shown as weight percent of a given element relative to the most dominant element present in the sample.

The average length distribution of the pristine and purified MWCNTs was evaluated using tapping mode Atomic Force Microscopy (AFM) performed in air (Asylum Research, AC240TS, 50 to 90 kHz). At least 3 scans of 10 μm × 10 μm were acquired for each of the sample being analyzed and a minimum of 30 individual MWCNTs were measured to obtain an average length distribution.

2.3 Functionalization of MWCNTs with fluorescent protein

Alexa 488-labeled Bovine Serum Albumin or Bovine Serum Albumin (Alexa-BSA, or BSA, Invitrogen) was covalently attached to purified MWCNTs using 1-ethyl-3-[3-dimethylaminopropyl] carbodiimide hydrochloride (EDC, Acros Organics) and N-hydroxysuccinimide (NHS, Pierce) chemistry.[18] Briefly, 2 mg of purified MWCNTs were dispersed in 160 mM EDC and 80 mM NHS (total volume of 2 mL in 2-(N-morpholino) ethanesulfonic acid sodium salt or MES, 50 mM, pH 4.7, (Sigma) for 15 min at room temperature with shaking at 200 rpm. EDC/NHS activated MWCNTs were subsequently filtered through a GTTP filter membrane, washed thoroughly with MES buffer, and immediately re-dispersed in 2 mL of 1 mg/mL protein solution in Phosphate Saline Buffer (PBS, Fisher), 100 mM, pH 7.4. The mixture was incubated for 3 h at room temperature with shaking at 200 rpm. Upon incubation, the resulting protein-based conjugates were filtered and washed extensively with PBS to remove any unbound protein. The supernatant and the first two washes were collected.

2.4 Protein loading

The amount of protein bound onto the purified MWCNTs (i.e., protein loading) was determined using standard bicinchoninic acid assay (BCA, Fisher).[18] For this, the working reagent was prepared by mixing 50 parts of reagent A (1000 μL), with 1 part of reagent B (50 μL) and subsequently mixing 1000 μl of that working reagent with 50 μL of either the collected supernatant or washes. The resulting solution was gently vortexed and incubated in a water bath at 37°C for 30 min. Upon time elapsed, the absorbance values were recorded on a Spectrophotometer (Evolution 300/600, Thermo Fisher) using 562 nm as reading wavelength. Control calibration curves were prepared using serial dilutions of protein in the working buffer. The relative amount of Alexa-BSA bound to the purified MWCNTs was estimated from the difference between the amount of protein initially added during the covalent incubation step and the amount of the protein removed in the supernatant and two washes as calculated by the BCA assay.

2.5 Dispersity analysis

The dispersity of MWCNTs or MWCNTs-functionalized with the protein was tested both in DI water and in Dulbecco's Modified Eagle Media (DMEM, Invitrogen) containing 10% Fetal Bovine Serum (FBS, Invitrogen). For this, MWCNTs were sonicated in the testing solution (for a final concentration of 5 mg/mL) and subsequently centrifuged at 3000 rpm for 5 min. Part of the corresponding supernatant (0.8 mL) was collected, filtered through a 0.2 μm GTTP filter membrane and then dried under vacuum. The amount of MWCNTs isolated on the filter was weighted and the dispersity was determined relative to the starting amount and volume used per individual sample.

2.6 Cell culture

Immortalized human bronchial epithelial cells (BEAS-2B, ATCC) were cultured in DMEM media containing 10% FBS, 0.1% L-glutamine and 1% penicillin/streptomycin (Invitrogen). Cells were maintained in a humidified atmosphere at 37°C and with 5% CO_2; for passaging, a 0.25% trypsin (Invitrogen) solution was used.

2.7 Fluorescence Activated Cell Sorting (FACS)

BEAS-2B cells were seeded for 24 h in T75 flasks (Fisher) at a density of 3.71×10^5 cells. Subsequently, the cells were exposed to 24 μg/cm^2 Alexa-BSA-MWCNTs conjugates dispersed in fresh media by brief sonication. Control samples, i.e., cells exposed to PBS, free Alexa-BSA at the equivalent amount to the Alexa-BSA amount loaded onto the MWCNTs, and cells exposed to unlabeled MWCNTs respectively, were performed in parallel. Upon 24 h incubation, the cells in each treatment group were washed with PBS, trypsinized (0.25% trypsin/EDTA, Fisher), suspended in DMEM containing 10% FBS and centrifuged at 1200 rpm for 5 min to remove free proteins, non-internalized, loosely bound nanotubes or conjugates. Upon centrifugation the samples were washed with PBS, fixed with 100 μL of 4% glutaraldehyde solution (Fisher) for 15 min at room temperature, and then extensively washed with PBS to remove free glutaraldehyde.

Analyses were performed on a FACS Caliber flow cytometer (Becton Dickinson). The forward scatter (FSC) and side scatter (SSC) were used to gate the samples to exclude the

cellular debris. FITC signal for the BSA-based conjugates used 488 nm excitation and 515 nm emission wavelengths. At least 30000 events were recorded for each sample and the data was analyzed and plotted using FlowJo v7.2.5 software.

2.8 Cell activity

BEAS-2B cells were seeded overnight at a density of 1.5×10^4 into a 96-well plate (Fisher) and exposed for 24, 48 and 72 h respectively to 24 μg/cm^2 purified MWCNTs dispersed by brief sonication in the culture media. Upon time elapse, 10 μl of tetrazolium salt (i.e., 2- (4-iodophenyl) - 3- (4-nitrophenyl) - 5- (2,4-disulfophenyl) -2H-tetrazolium also known as WST-1, Roche), was added to each well and the plate was incubated for 2 h at room temperature. Changes in the color of the individual wells were based on the cells ability to cleave WST-1 salt to farmazan in the presence of the enzyme dehydrogenase and were assessed using a BioTek 96 plate reader (BioTek) and 450 nm absorbance. The changes are reported as percentage relative activity of exposed versus unexposed cells.

2.9 Cell cycle analysis

BEAS-2B cells were seeded overnight in 6 well plates (Fisher) at a concentration of 3×10^5 cells/well, and exposed for 24 h to 24 μg/cm^2 purified MWCNTs dispersed in cellular media. Following exposure to MWCNTs, cells were trypsinized, collected, washed twice with PBS, centrifuged at 1500 rpm for 6 min and fixed overnight in 2 mL 70% ethanol (Fisher) at −20°C. Subsequently, the cells were washed again, suspended in 0.2% Tween 20 (Sigma Chemicals) for 15 min, treated with 10 μl 0.05% RNase for 15 min and stained with 30 μl propidium iodide (Sigma). Changes in DNA content were determined using BD LSR Fortessa Flow cell analyzer (BD Biosciences), and the BD FACS Diva (Verity Software House) and FlowJo V10.0.7 (Tree Star Inc.) software. The forward scatter (FSC) and side scatter (SSC) were used to gate the majority of the cell population; 20000 events were collected for each sample. The selection of the cells was based on knowing that in the G0/G1 phase (before DNA synthesis) cells have a defined amount of DNA (i.e., a diploid chromosomal DNA content) and double that amount in G2 or M phases (G2/M, i.e., a tetraploid chromosomal DNA content). Complementary, during the S phase (DNA synthesis), cells contain between one to two DNA levels.

2.10 Cell nanomechanical properties analysis

BEAS-2B cells were seeded overnight in 50 mm × 9 mm parallel culture Petri dishes (BD Biosciences) at a density of 1×10^5 cells per dish. Cells were exposed to 24 μg/cm^2 purified MWCNTs for 24 h. MFP-3D-BIO AFM (Asylum Research, TE2000-U) was used to evaluate individual cell Young modulus. Individual cells were selected using optical microscopy and scanned in contact mode in liquid using an Olympus TR400-PB cantilever; the spring constant of the cantilever was measured before each experiment by using a thermal tuning method.[19] The trigger force was in the nanonewtons range (i.e., 2.3–4.0 nN) while the fitting percentage considered for the data analysis was 90%. Analysis was based on the Sneddon's modification of the Hertz model for a four-sided pyramid[20, 21] with the stiffness being calculated knowing the indentation of the tip and the Poisson's ratio of the cell (v=0.5).[21]

2.10 Statistical analysis

For the FTIR, the experiments were repeated at least three times each with two replicates for a total of 6 replicates.

Statistical analyses for the biomechanical and cell cycle experiments were performed with SAS/STAT software (v9.2) for Windows.

Two-way analysis of variance (ANOVA) and unpaired two-tailed Student's t-test by SigmaPlot 10.0 (Systat Software Inc.) were used to study the effects of MWCNTs on cellular activity and the BSA loading. Experiments were repeated at least three times each with three replicates for a total of 9 replicates.

Differences were considered significant for $p^* < 0.05$.

3. Results and Discussion

MWCNTs purification in sulfuric/nitric acids mixture[22] was used to eliminate possible catalyst precursors otherwise present during the nanotube synthesis.[11] Pristine and purified MWCNTs samples were investigated using Scanning Electron Microscopy (SEM), Atomic Force Microscopy (AFM), Attenuated Total Reflection Fourier Transform Infrared Spectroscopy (ATR-FTIR), and Energy Dispersive X-ray spectroscopy (EDX) spectroscopy for their physical and chemical properties. SEM analysis showed that purification did not significantly change the morphology of the MWCNTs (Figure S1), while AFM analysis showed that the average length of the purified MWCNTs (792±254 nm)was about 81% shorter than that of pristine MWCNTs (4261±2354 nm; Table S1), which is consistent with previous reports.[11]

Research has shown that shortening of the MWCNTs leads to formation of chemical groups such as COOH,[23] OH,[24] and CO[12] at the nanotube defect sites. Our ATR-FTIR analysis confirmed the presence of the O-containing functional groups (Figure 1a). The peak at 3370 cm^{-1} was attributed to the O-H stretching vibration[25] while the peak around 1670 cm^{-1} was associated with the C=O stretching vibration.[26] In addition, the small peak at around 1330 cm^{-1} was a result of the O-H bending vibration,[27] and the wide range of peaks between 1000–1250 cm^{-1} were associated with the C-O stretching vibrations. [28] The peak around 2000 cm^{-1} was previously associated with MWCNTs functionalization with O-containing groups.[29, 30] The increase in O-containing functional groups and removal of metal catalysts was confirmed by EDX (Table S2), with the analysis also showing a decrease in the Fe and Cu contents for the purified MWCNTs relative to their pristine counterparts.[11]

The solubility of pristine, purified and protein-MWCNTs conjugates was also tested; well-dispersed MWCNTs are required to eliminate mass transfer limitations when studying the interactions of such nanomaterials with cellular systems.[31, 32] Analysis showed that purified MWCNTs were highly dispersed, especially in DMEM media (Table S3), presumably due to the: (1) formation of carboxylate anions, and/or (2) the hydrodynamic size of the purified nanotube. For the first, the negative charges or the carboxylate anions resulted upon nanotube treatment with the acids mixture could potentially lead to strong electrostatic repulsion between individual MWCNTs,[33, 34] while the presence of proteins and amino

acids in the DMEM media can aid to the increased dispersity.[35] For the second, the shorter nanotubes (as shown by AFM) have smaller hydrodynamic radius and thus end-to-end distances than their pristine counterparts.[36]

Human bronchial respiratory epithelial cells (BEAS-2B) were exposed to 24 μg/cm^2 of purified MWCNTs covalently functionalized with Alexa-BSA for 24 h; uptake of fluorescently labeled MWCNTs was evaluated as a change in the forward scatter (FSC) and side scatter (SSC) of the exposed cells by using a Fluorescence Assisted Cell Sorting (FACS) machine. Cells exposed to purified MWCNTs alone, cells exposed to free Alexa-BSA, and cells exposed to media were used as controls. Figure 1b shows a significantly higher FITC signal for cells treated with Alexa-BSA-MWCNTs conjugates relative to all the control experiments. The higher signal was consistent with internationalization of the labeled MWCNTs, with the relatively lower intensity observed for the cells exposed to free Alexa-BSA presumably due to the increased Alexa-BSA susceptibility for proteasomal degradation upon its uptake relatively to the more stable MWCNTs-immobilized Alexa-BSA.[37–39]

To investigate the cellular activity upon uptake of MWCNTs, the exposed cells were assessed using WST-1 assay to measure the mitochondrial dehydrogenase activity (Figure 1c). Mitochondria are relatively sensitive organelles known to respond to cellular stresses caused by the uptake of CNTs.[40] WST-1 was preferred to the MTT assay due to existing concerns regarding CNTs interaction with the nonsoluble tetrazolium salt formed in the later.[41] Our results showed a significant reduction in the cellular activity of the cells exposed for 24, 48, and 72 h to the purified MWCNTs. The reduction was presumably due to the internalized MWCNTs initiating mitochondrion stress that could have led to increased concentrations of cytoplasmic (Ca^{2+})[42] and changes in the mitochondrial permeability transition membrane pores (MPTPs) potential.[43] Studies have shown that when MPTPs are open, the cytochrome Ca^{2+} pro-apoptotic factor (located in the inner membrane of the mitochondria) and Ca^{2+} diffuse into the mitochondrial matrix and could trigger caspases-8 -9 and -3 signaling eventually leading to cell apoptosis.[42, 44]

Changes in the cellular activity observed upon exposure to purified MWCNTs were further translated into changes in the cell cycle progression;[45] Figure 2 shows cell cycle arrest at the G1/S phase 24 h post-exposure. Specifically, gating of the cell population (Figure 2a) or single cells (Figure 2b) showed that cells exposed to purified MWCNTs had a statistically significant increase in G1 (gap) phase (13±5.35%) and a significant decrease in S (synthesis) phase (25±6.42%; Figure 2d), both relative to controls ($p^* < 0.05$; Figure 2c) (Table S4). The increase in G1 could be associated with an extensive change in the DNA content, cell volume, and/or increased synthesis of mRNA and proteins.[46] The change in the S phase could be associated with a decrease of available cellular DNA[47] based on the known affinity of CNTs for nuclei acids.[48] The observed changes in the cell cycle progression could lead to defects in DNA synthesis and chromosome segregation and hint to the possibility of MWCNTs to induce genotoxicity[8] thus complementing previous reports showing CNT-induced chromosomal damage,[49] generation of reactive oxygen species (ROS),[50] or multipolar mitotic spindles.[8, 51]

Changes in the cellular activity and cell cycle progression were complemented by changes in the cell biomechanics (Figure 3). Previous studies have shown that changes in cellular biomechanics with an increase in cell deformability correlate with the progression of a cell to a transformed phenotype, i.e., from a benign to a malignant one.[52] Further, previous research showed that the AFM can be used to investigate biomechanical properties of fixed cells treated with MWCNTs[15] or to identify cancer cells from a mixture with normal cells,[53] with reports showing that for an applied force above 7 nN the elastic modulus of a single cell is relatively independent of the tip indentation.[54]

The elastic modulus distributions of control and MWCNTs-exposed live cells (both cell bodies and cell nuclei) are shown in Table 1, with a typical example of force-indentation (F-Z) curve recorded at the nucleus region shown in Figure 3a. Compared to the control cells, the cells exposed to purified MWCNTs showed less deformation suggesting a change in their elastic properties, especially at their nuclear regions where the engaging of the AFM tip was weaker than at the cell edges typically consisting concentrated cytoskeleton fibers.[55] Comparison between the elastic modulus of purified MWCNTs-exposed live cells and control live cells showed a relatively narrow Young modulus distribution for their nucleus regions (0–6kPa) and a much wider distribution for the whole cell bodies (0–12kPa); higher elastic modulus (~20 kPa) was observed at the cell periphery and was attributed to the effects induced by the plastic substrate.[56] Specifically, the average Young moduli for the whole cell bodies were 2.72±0.96 and 3.84±1.12 kPa for control and exposed live cells respectively, while the average Young moduli at their nuclei regions were 1.58±0.67 and 2.20±0.59 kPa respectively (Figure 3b).

Based on the observed live cell changes, we propose that cellular uptake of the purified MWCNTs induces a series of concurrent processes (i.e., changes in cellular activity and biomechanical properties), which are function of the nanomaterial physical and chemical properties. Such changes could possibly induce cytoskeletal filament reorganization which could lead to increased cellular rigidity, and possible inhibition and/or blockage of intracellular biomolecular transport or cell cycle progression (Figure 4). Preliminary research has shown that exposure to MWCNTs led to their cellular integration either into the endosomal structures[57] or into cytoskeletal filaments[51] leading to the formation of hybrid-MWCNTs filaments.[8, 15] Interestingly, the elastic moduli for control BEAS-2B cells were higher than previously reported (~75%)[55] presumably due to variation in the cell culture[58] or nanoindentation and fixation conditions.[54] Our data supports recent evidence that relates MWCNTs cytotoxic and genotoxic effects to both their physical and chemical properties[59] and suggests that occupational exposure to such nanomaterials needs to be fully assessed before implementation in biomedical-related applications is sought.

4. Conclusions

Our results showed that purified MWCNTs exposure affects the mitochondrial activity, cell biomechanical properties and cell cycle progression in human lung epithelial cells. The analysis further hints at a possible cyto and genotoxic synergism associated with the cellular exposure to MWCNTs which could potentially induce cell transformation and thus cancer progression.

Supplementary Material

Refer to Web version on PubMed Central for supplementary material.

Acknowledgments

Support for this research was provided through Nano SAFE, National Science Foundation grant EPS-1003907, NORA 927000Y and the National Institute of Health (NIH; R01-ES022968).

Authors acknowledge the use of the WVU Shared Research Facilities and the help of Jeremy Hardinger with EDX analysis. Flow cytometry experiments were performed in the Flow Cytometry Core Facility at WVU; the core is in part supported by the National Institute of Health equipment grant number S10OD016165 and the Institutional Development Award (IDeA) from the National Institute of General Medical Sciences of the National Institutes of Health under grant numbers P30GM103488 (CoBRE) and P20GM103434 (INBRE). The authors acknowledge the support and expertise of Dr. Karen Martin, the director of the Core Facility.

References

1. Delogu LG, Vidili G, Venturelli E, Menard-Moyon C, Zoroddu MA, Pilo G, Nicolussi P, Ligios C, Bedognetti D, Sgarrella F, Manetti R, Bianco A. P Natl Acad Sci USA. 2012; 109:16612–16617.
2. Das M, Singh RP, Datir SR, Jain S. Mol Pharmaceut. 2013; 10:3404–3416.
3. Tsai HC, Lin JY, Maryani F, Huang CC, Imae T. Int J Nanomed. 2013; 8:4427–4440.
4. Li J, Pant A, Chin CF, Ang WH, Menard-Moyon C, Nayak TR, Gibson D, Ramaprabhu S, Panczyk T, Bianco A, Pastorin G. Nanomedicine-Uk. 2014 in press.
5. Jiang L, Liu TB, He H, Pham-Huy LA, Li LL, Pham-Huy C, Xiao DL. J Nanosci Nanotechnol. 2012; 12:7271–7279. [PubMed: 23035463]
6. Sager TM, Wolfarth MW, Andrew M, Hubbs A, Friend S, Chen TH, Porter DW, Wu NQ, Yang F, Hamilton RF, Holian A. Nanotoxicology. 2014; 8:317–327. [PubMed: 23432020]
7. Aneta Fraczek-Szczypta EM, Syeda Tahmina Bahar, Misra Anil, Alavijeh Mohammad, Adu Jimi, Blazewicz Stanislaw. J Nanopart Res. 2012; 14:1181-1–1181-14. [PubMed: 23087595]
8. Siegrist KJ, Reynolds SH, Kashon ML, Lowry DT, Dong CB, Hubbs AF, Young SH, Salisbury JL, Porter DW, Benkovic SA, McCawley M, Keane MJ, Mastovich JT, Bunker KL, Cena LG, Sparrow MC, Sturgeon JL, Dinu CZ, Sargent LM. Part Fibre Toxicol. 2014; 11:1–15. [PubMed: 24382024]
9. Pacurari M, Yin XJ, Ding M, Leonard SS, Schwegler-Berry D, Ducatman BS, Chirila M, Endo M, Castranova V, Vallyathan V. Nanotoxicology. 2008; 2:155–170.
10. Erdely A, Dahm M, Chen BT, Zeidler-Erdely PC, Fernback JE, Birch ME, Evans DE, Kashon ML, Deddens JA, Hulderman T, Bilgesu SA, Battelli L, Schwegler-Berry D, Leonard HD, McKinney W, Frazer DG, Antonini JM, Porter DW, Castranova V, Schubauer-Berigan MK. Part Fibre Toxicol. 2013; 10:1–14. [PubMed: 23305071]
11. Dong CB, Campell AS, Eldawud R, Perhinschi G, Rojanasakul Y, Dinu CZ. Appl Surf Sci. 2013; 264:261–268.
12. Rike Yudianti HO, Saito Yukie, Iwata Tadahisa, Azuma Jun-ichi. Open Mater Sci. 2011; 5:242–247.
13. Koyama S, Kim YA, Hayashi T, Takeuchi K, Fujii C, Kuroiwa N, Koyama H, Tsukahara T, Endo M. Carbon. 2009; 47:1365–1372.
14. Murphy FA, Schinwald A, Poland CA, Donaldson K. Part Fibre Toxicol. 2012; 9:1–15. [PubMed: 22239852]
15. Dong CB, Kashon ML, Lowry D, Dordick JS, Reynolds SH, Rojanasakul Y, Sargent LM, Dinu CZ. Adv Healthcare Mater. 2013; 2:945–951.
16. Rogers-Nieman GM, Dinu CZ. Wiley Interdiscip Rev Nanomed Nanobiotechnol. 2014; 6:327–337. [PubMed: 24715535]
17. Mercer RR, Scabilloni JF, Hubbs AF, Battelli LA, McKinney W, Friend S, Wolfarth MG, Andrew M, Castranova V, Porter DW. Part Fibre Toxicol. 2013; 10:2–11. [PubMed: 23388071]

18. Campbell AS, Dong C, Meng F, Hardinger J, Perhinschi G, Wu N, Dinu CZ. ACS Appl Mater Interfaces. 2014; 6:5393–5403. [PubMed: 24666280]
19. Ohler B. Rev Sci Instrum. 2007; 78:063701-1–063701-5. [PubMed: 17614610]
20. Rotsch C, Jacobson K, Radmacher M. P Natl Acad Sci USA. 1999; 96:921–926.
21. Radmacher M, Fritz M, Kacher CM, Cleveland JP, Hansma PK. Biophys J. 1996; 70:556–567. [PubMed: 8770233]
22. Scheibe B, Borowiak-Palen E, Kalenczuk RJ. Mater Charact. 2010; 61:185–191.
23. Datsyuk V, Kalyva M, Papagelis K, Parthenios J, Tasis D, Siokou A, Kallitsis I, Galiotis C. Carbon. 2008; 46:833–840.
24. Qu ZH, Wang GJ. J Nanosci Nanotechnol. 2012; 12:105–111. [PubMed: 22523952]
25. Singh BP, Singh D, Mathur RB, Dhami TL. Nanoscale Res Lett. 2008; 3:444–453.
26. Teng LH, Tang TD. J Zhejiang Univ-Sc A. 2008; 9:720–726.
27. Moreno-Castilla C, Lopez-Ramon MV, Carrasco-Marin F. Carbon. 2000; 38:1995–2001.
28. Wang L, Ge L, Rufford TE, Chen JL, Zhou W, Zhu ZH, Rudolph V. Carbon. 2011; 49:2022–2032.
29. Wei J, Lv R, Guo N, Wang HG, Bai X, Mathkar A, Kang FY, Zhu HW, Wang KL, Wu DH, Vajtai R, Ajayan PM. Nanotechnology. 2012; 23:1–5.
30. Hoa LQ, Vestergaard MC, Yoshikawa H, Saito M, Tamiya E. J Mater Chem. 2012; 22:14705–14714.
31. Gliga AR, Skoglund S, Wallinder IO, Fadeel B, Karlsson HL. Part Fibre Toxicol. 2014; 11:1–17. [PubMed: 24382024]
32. Emilie Brun FB, Veronesi Giulia, Fayard Barbara, Sorieul Stéphanie, Chanéac Corinne, Carapito Christine, Rabilloud Thierry, Mabondzo Aloïse, Herlin-Boime Nathalie, Carrière Marie. Part Fibre Toxicol. 2014; 11:1–16. [PubMed: 24382024]
33. Shieh YT, Liu GL, Wu HH, Lee CC. Carbon. 2007; 45:1880–1890.
34. Li RB, Wang X, Ji ZX, Sun BB, Zhang HY, Chang CH, Lin SJ, Meng H, Liao YP, Wang MY, Li ZX, Hwang AA, Song TB, Xu R, Yang Y, Zink JI, Nel AE, Xia T. ACS Nano. 2013; 7:2352–2368. [PubMed: 23414138]
35. Voge CM, Johns J, Raghavan M, Morris MD, Stegemann JP. J Biomed Mater Res A. 2013; 101A: 231–238. [PubMed: 22865813]
36. He FA, Fan JT. Mater Sci Tech-Lond. 2013; 29:1423–1429.
37. Lecker SH, Goldberg AL, Mitch WE. J Am Soc Nephrol. 2006; 17:1807–1819. [PubMed: 16738015]
38. Weill CO, Biri S, Adib A, Erbacher P. Cytotechnology. 2008; 56:41–48. [PubMed: 19002840]
39. Martensen PM, Justesen J. Biotechniques. 2001; 30:782-+. [PubMed: 11314261]
40. Chen T, Zang JJ, Wang HF, Nie HY, Wang X, Shen ZL, Tang SC, Yang JL, Jia G. J Nanosci Nanotechnol. 2012; 12:8008–8016. [PubMed: 23421171]
41. Worle-Knirsch JM, Pulskamp K, Krug HF. Nano Lett. 2006; 6:1261–1268. [PubMed: 16771591]
42. Wang X, Guo J, Chen T, Nie H, Wang H, Zang J, Cui X, Jia G. Toxicol In Vitro. 2012; 26:799–806. [PubMed: 22664788]
43. Lemasters JJ, Nieminen AL, Qian T, Trost LC, Elmore SP, Nishimura Y, Crowe RA, Cascio WE, Bradham CA, Brenner DA, Herman B. Bba-Bioenergetics. 1998; 1366:177–196. [PubMed: 9714796]
44. Zhong W, Chen X, Jiang P, Wan JMF, Qin P, Yu ACH. Ultrasound Med Biol. 2013; 39:2382–2392. [PubMed: 24063957]
45. Berridge MJ. Cell Signal Bio. 2012:1–63. Module 1.
46. Bertoli C, Skotheim JM, de Bruin RAM. Nat Rev Mol Cell Bio. 2013; 14:518–528. [PubMed: 23877564]
47. Bellucci S, Dinicola S, Coluccia P, Bizzarri M, Catizone A, Micciulla F, Sacco I, Ricci G, Cucina A. Int Semiconduct Con. 2012; 2:37–42.
48. Roxbury D, Tu XM, Zheng M, Jagota A. Langmuir. 2011; 27:8282–8293. [PubMed: 21650196]
49. Migliore L, Saracino D, Bonelli A, Colognato R, D'Errico MR, Magrini A, Bergamaschi A, Bergamaschi E. Environ Mol Mutagen. 2010; 51:294–303. [PubMed: 20091701]

50. He XQ, Young SH, Schwegler-Berry D, Chisholm WP, Fernback JE, Ma Q. Chem Res Toxicol. 2011; 24:2237–2248. [PubMed: 22081859]
51. Rodriguez-Fernandez L, Valiente R, Gonzalez J, Villegas JC, Fanarraga ML. ACS Nano. 2012; 6:6614–6625. [PubMed: 22769231]
52. Kumar S, Weaver V. Cancer Metast Rev. 2009; 28:113–127.
53. Cross SE, Jin YS, Rao J, Gimzewski JK. Nat Nanotechnol. 2007; 2:780–783. [PubMed: 18654431]
54. Dokukin ME, Guz NV, Sokolov I. Biophys J. 2013; 104:2123–2131. [PubMed: 23708352]
55. Alcaraz J, Buscemi L, Grabulosa M, Trepat X, Fabry B, Farre R, Navajas D. Biophys J. 2003; 84:2071–2079. [PubMed: 12609908]
56. Rheinlaender J, Geisse NA, Proksch R, Schaffer TE. Langmuir. 2011; 27:697–704. [PubMed: 21158392]
57. Mu QX, Broughton DL, Yan B. Nano Lett. 2009; 9:4370–4375. [PubMed: 19902917]
58. Nikkhah M, Strobl JS, Schmelz EM, Agah M. J Biomech. 2011; 44:762–766. [PubMed: 21109247]
59. Shen MW, Wang SH, Shi XY, Chen XS, Huang QG, Petersen EJ, Pinto RA, Baker JR, Weber WJ. J Phys Chem C. 2009; 113:3150–3156.

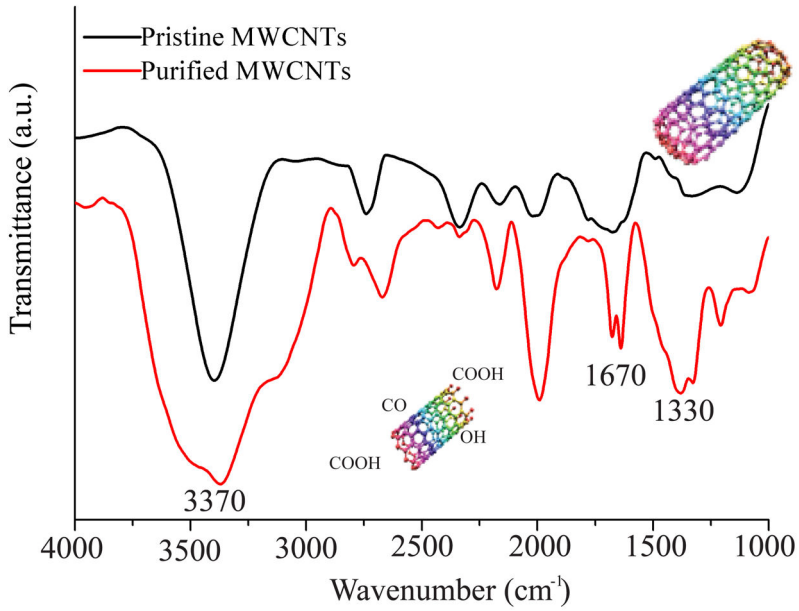

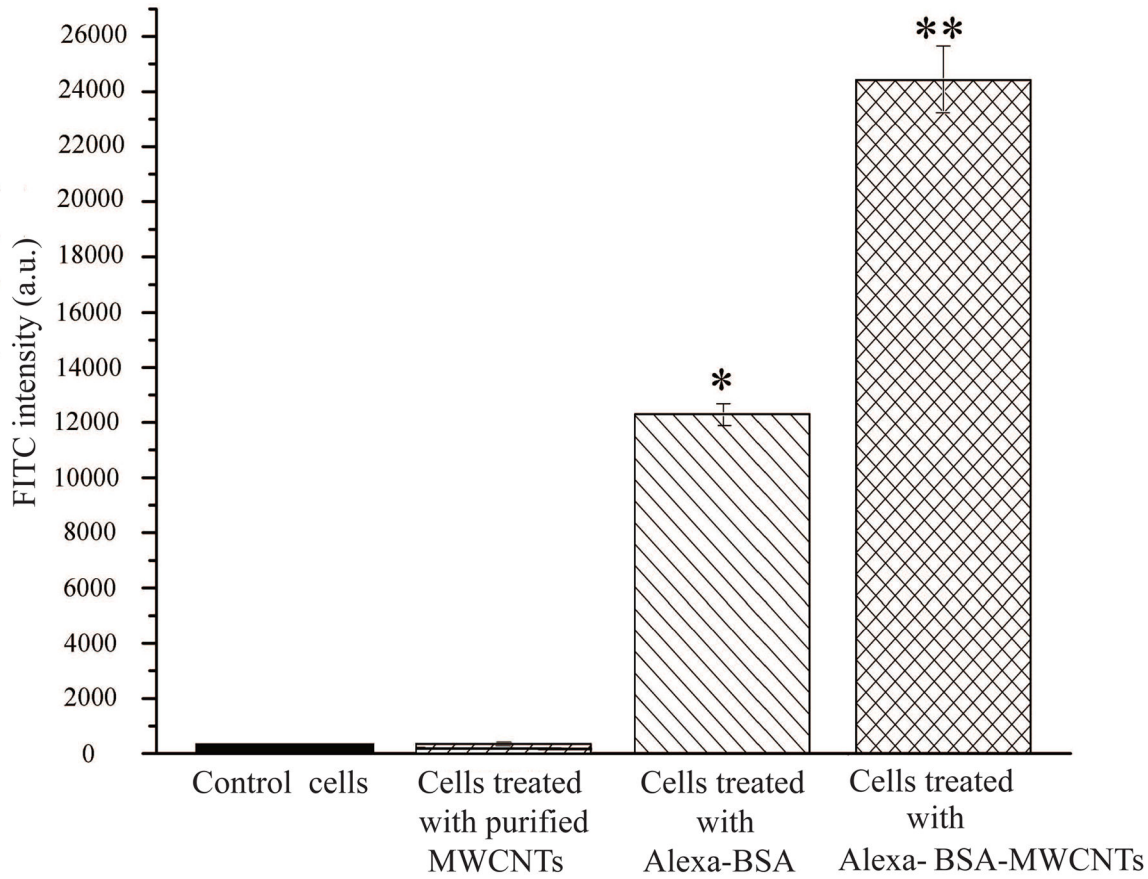

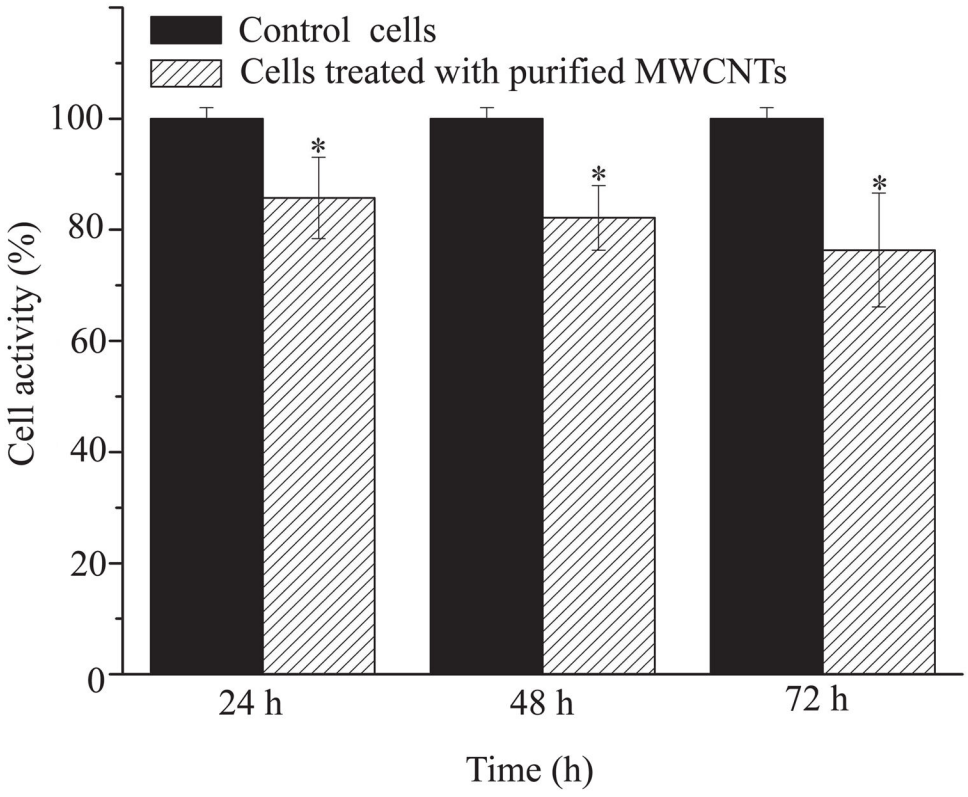

Figure 1.

(a) FTIR spectrum of pristine MWCNTs and purified MWCNTs (n=6). (b) FITC intensity of control cells, purified MWCNTs, BEAS-2B cells treated with Alexa-BSA and cells treated with Alexa-BSA-MWCNTs conjugates (n=9). (c) (%) Changes in the activity of the cells exposed to 24 μg/cm^2 purified MWCNTs. Changes are considered significant for $p^*<0.05$.

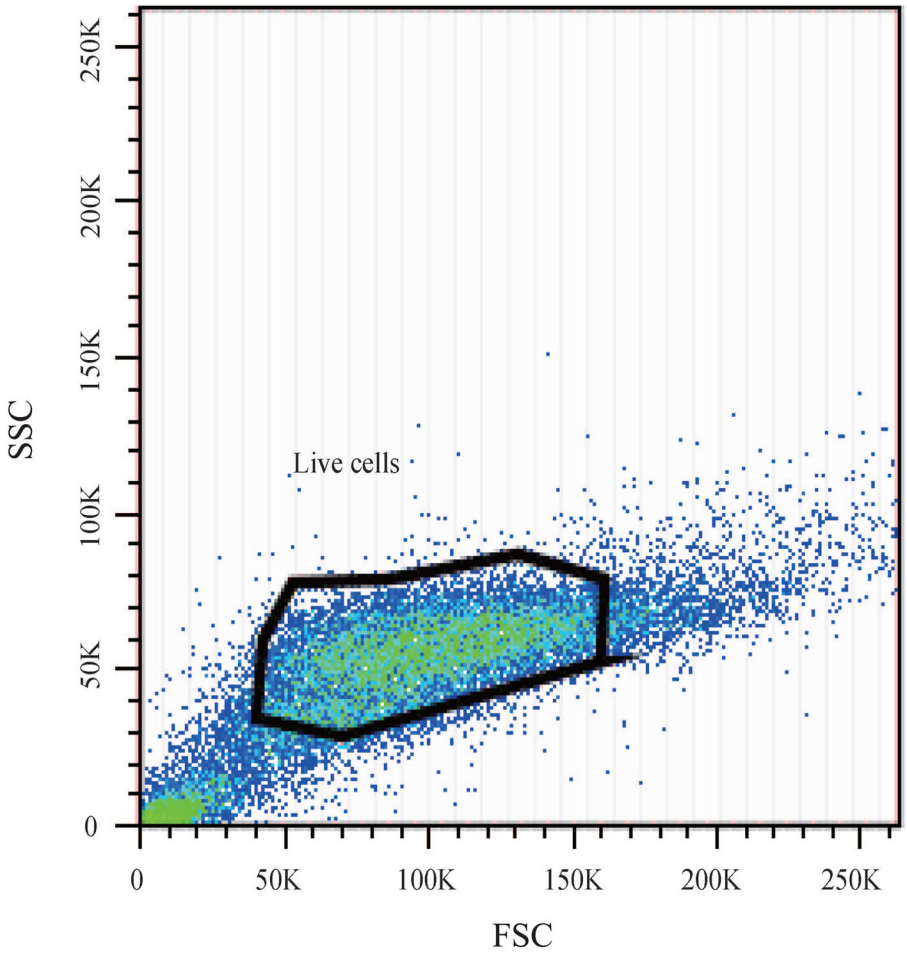

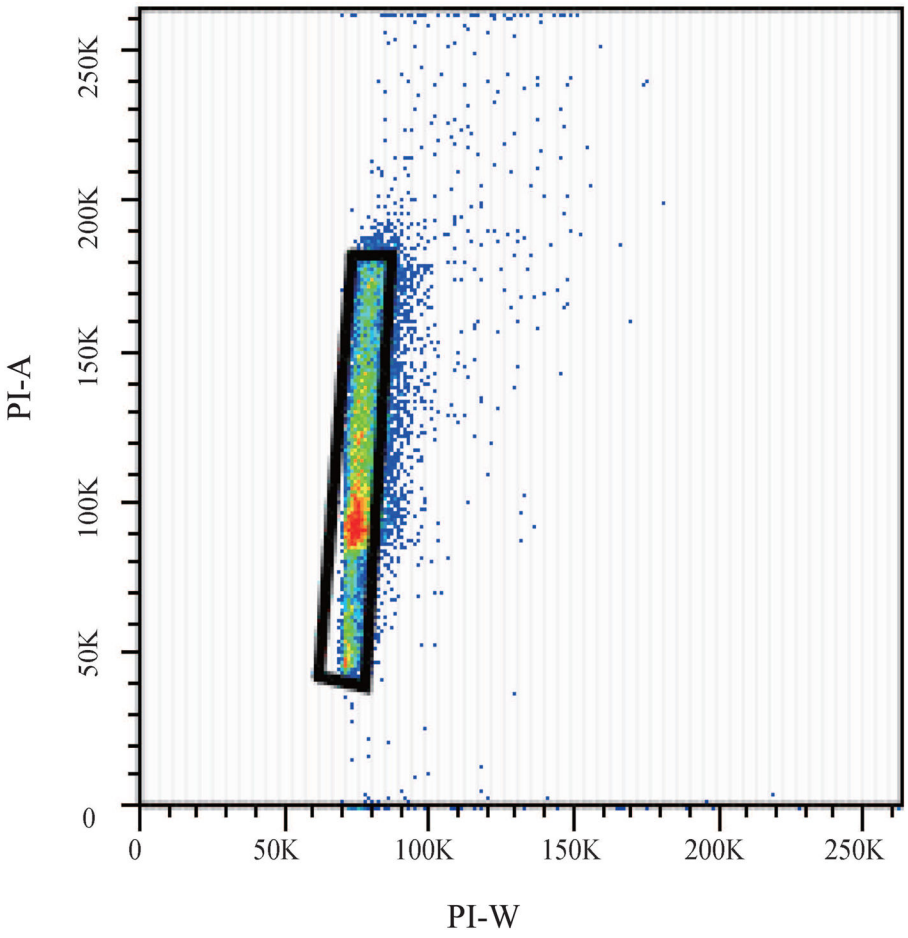

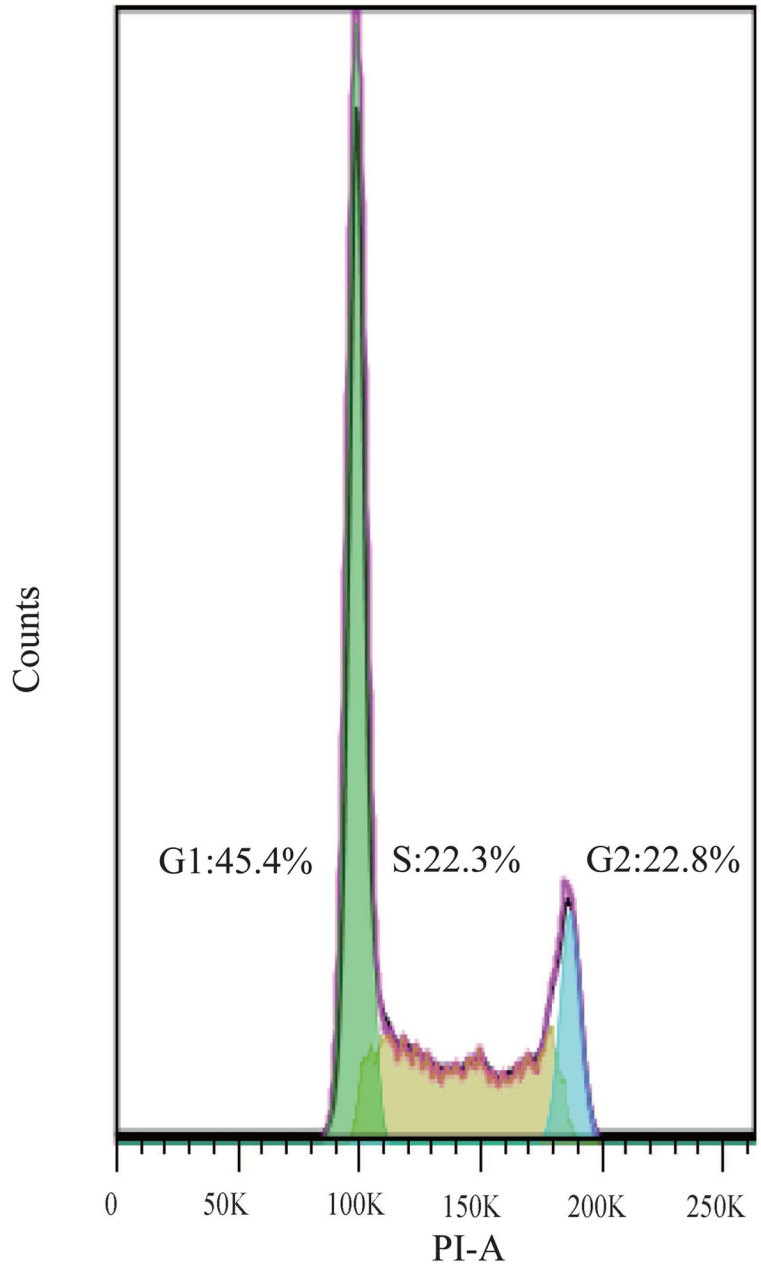

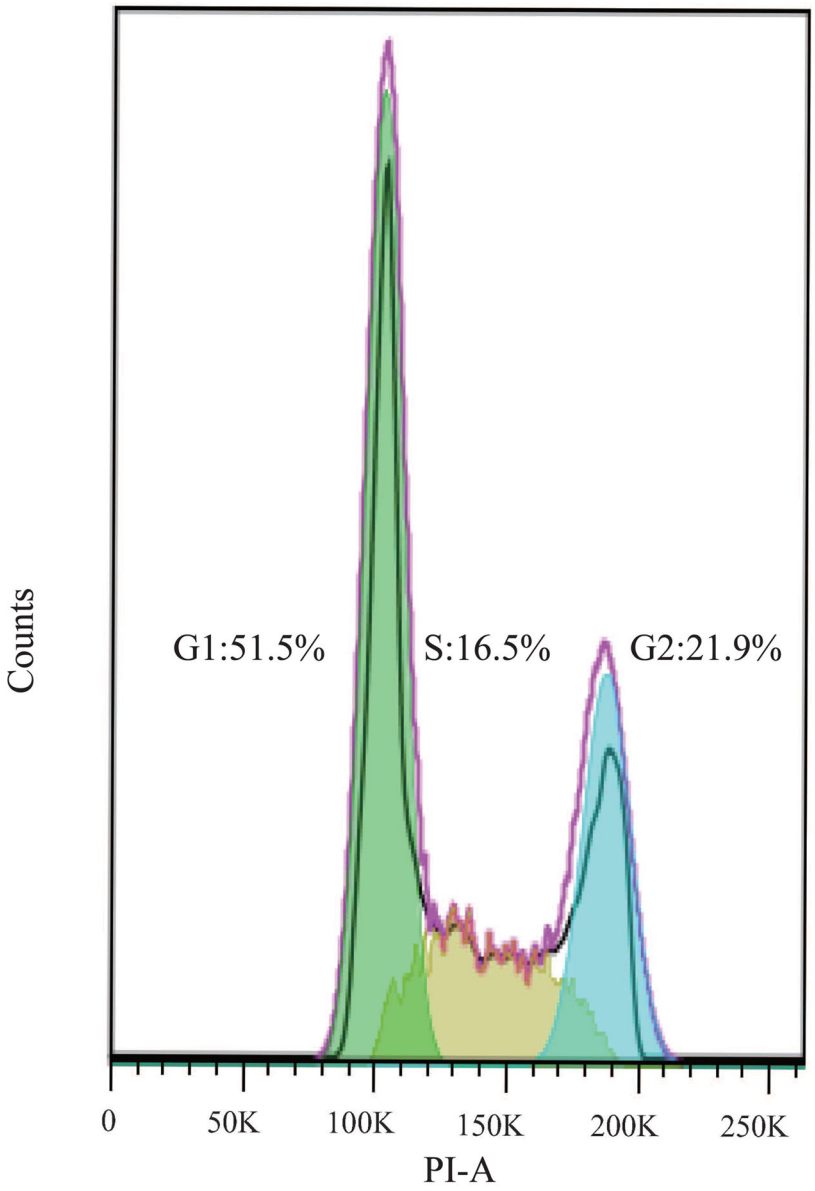

Figure 2.

Fluorescence Activated Cell Sorting (FACS) was used to evaluate the changes in cell cycle upon exposure to purified MWCNTs; PI-stained BEAS-2B cells were used. (a) Forward scatter (FSC) and side scatter (SSC) 2D-plot showing a representative gating of the live cell population. (b) Scatter plot selection of single cells; representative gating. (c) Cell cycle analysis of controls cell and (d) cells exposed to purified MWCNTs respectively.

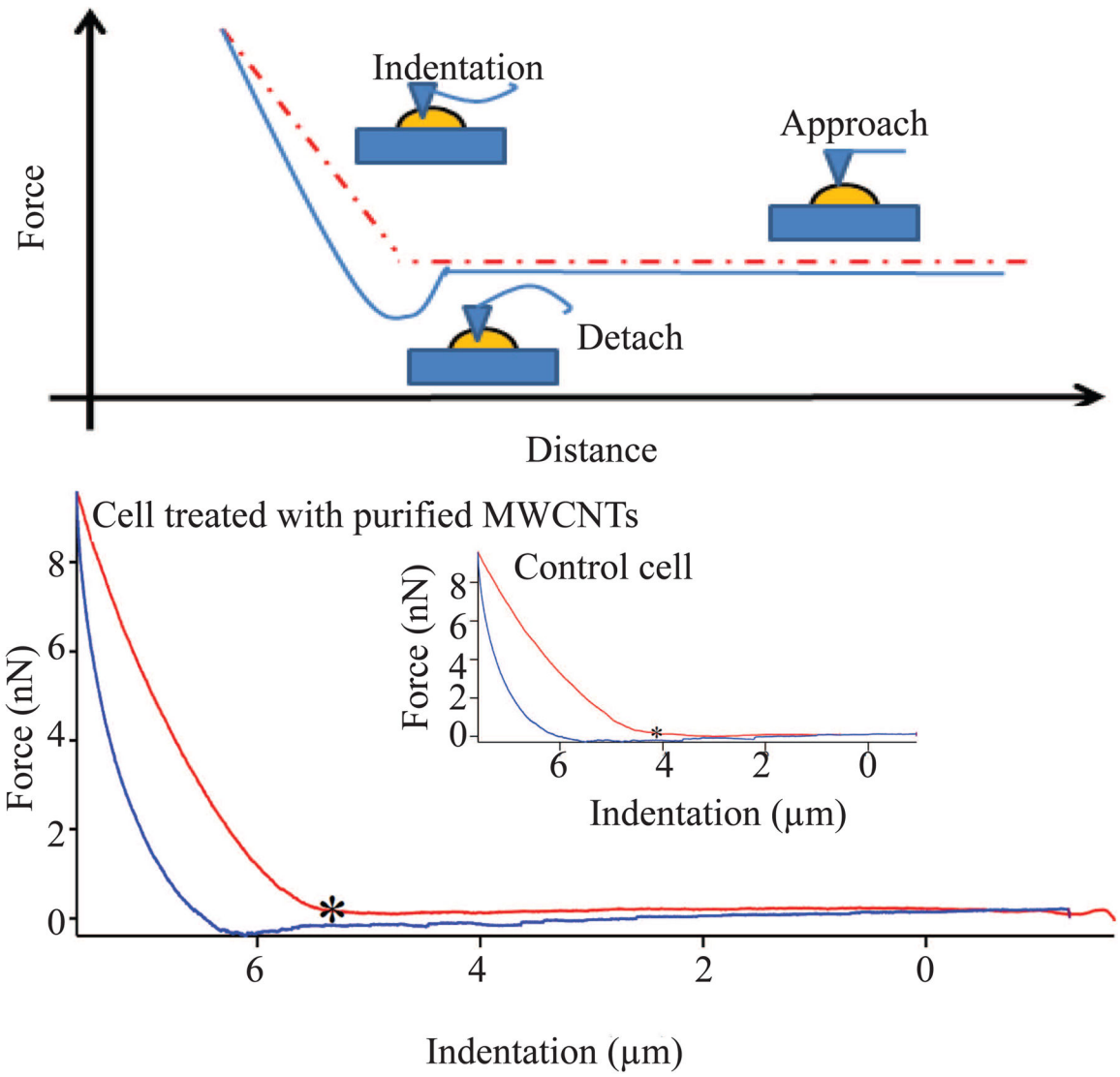

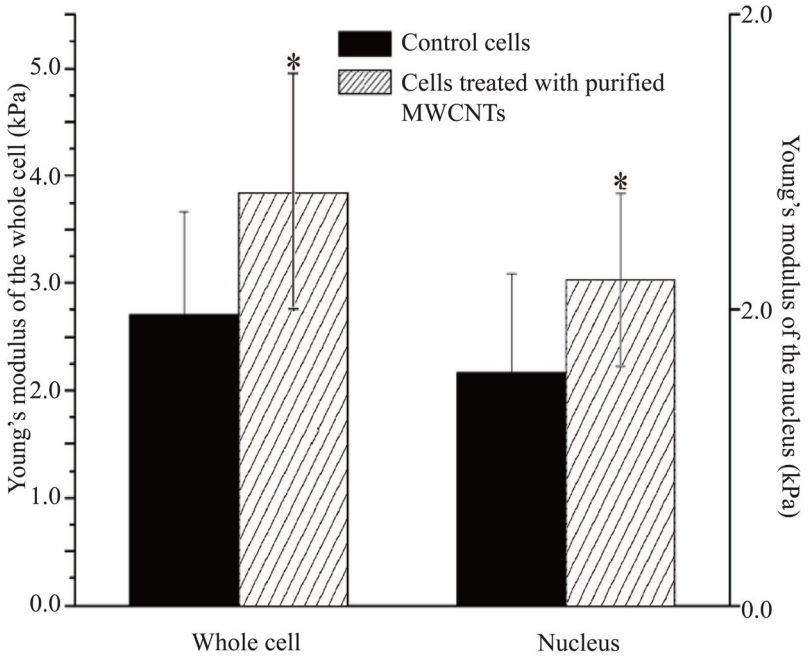

Figure 3.

(a) Schematic diagram of the force–indentation profile of control and cell exposed to purified MWCNTs. The red curve follows the approach of the tip to the plastic surface while the blue curve follows the detachment of the tip from the surface. "*" indicates the point at which the tip deflected from the surface to allow acquisition of the force-indentation measurement profile. (b) Average Young modulus of the whole live cell and the nucleus region of control and live cells exposed to purified MWCNTs for 24 h. All differences were considered statistically significant for $p^* < 0.05$.

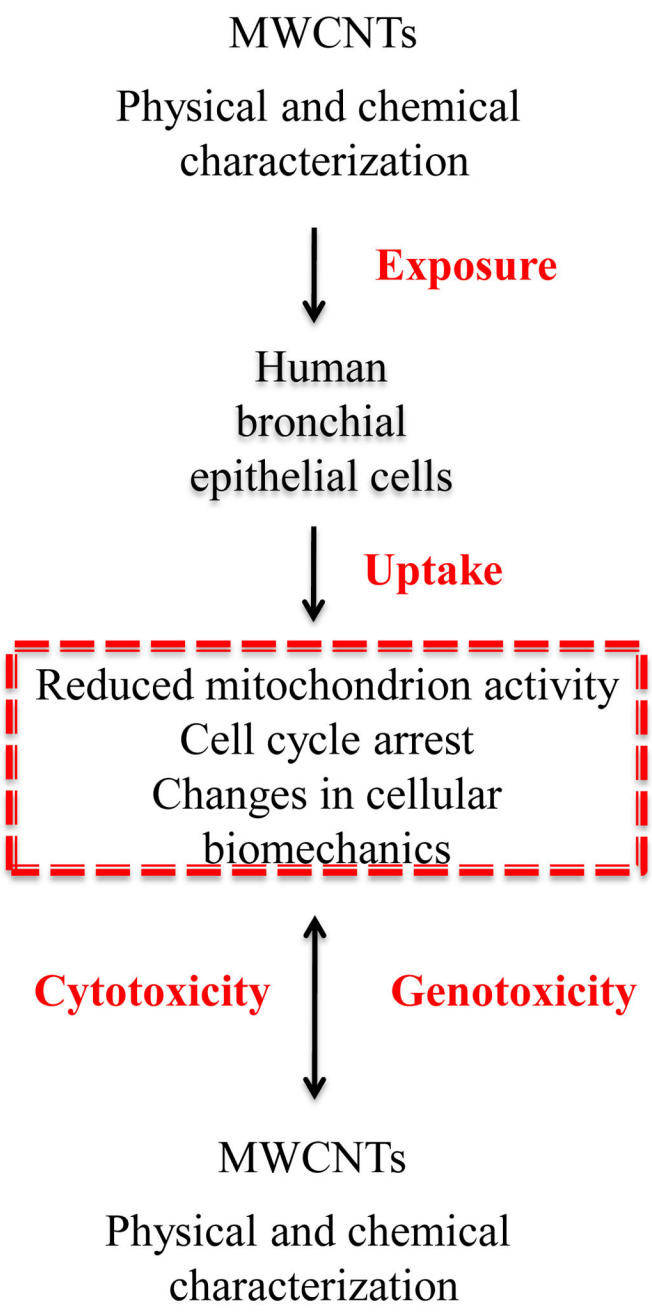

Figure 4.
Exposure to purified MWCNTs induced cyto-genotoxic effects by reducing cellular activity, changing cell's biomechanical properties and disrupting the cell cycle.

Table 1

Young's modulus distribution of control live cells and live cells exposed to purified MWCNTs.

Group	Counts	0–2kPa	2–4kPa	4–6kPa	6–10kPa	>10kPa
Control (whole cells)	380	50.79%	31.84%	10.79%	6.05%	0.53%
Cells incubated with purified MWCNTs (whole cells)	475	37.89%	35.58%	14.32%	7.79%	0.62%
Control (nucleus region)	104	76.92%	21.53%	1.55%	0%	0%
Cells incubated with purified MWCNTs (nucleus region)	122	57.38%	30.07%	12.55%	0%	0%